Earthquakes and Structures, *Vol. 8, No. 5 (2015) 1091-1111*
DOI: http://dx.doi.org/10.12989/eas.2015.8.5.1091

Simplified procedure for seismic analysis of base-isolated structures

Mohammed H. Serror*, Sherif O. El-Gazzar[a] and Sherif A. Mourad[b]

Department of Structural Engineering, Faculty of Engineering, Cairo University, Egypt

(Received July 28, 2014, Revised October 11, 2014, Accepted October 17, 2014)

Abstract. Base isolation is an effective method for protecting structures against earthquake hazard. It elongates the period of vibration and introduces supplemental damping to the structural system. The stiffness, damping and displacement are coupled forcing the code seismic design procedure to be unnecessarily complicated. In addition, the force reduction factor -a key parameter in the design procedure- has not been well addressed by seismic design codes at the high levels of damping due to the pronounced difference between pseudo and actual accelerations. In this study, a comparison has been conducted to evaluate eight different methods, in the literature, for calculating the force reduction factor due to damping. Accordingly, a simplified seismic analysis procedure has been proposed based on the well documented N2 method. Comprehensive analysis has been performed for base-isolated structure models for direct application and verification of the proposed procedure. The results have been compared with those of the European code EC8, the nonlinear time history analysis and investigations in the literature, where good agreement has been reported. In addition, a discussion has been elaborated for the resulted response of the base-isolated structure models with respect to the dynamic characteristics of the base isolation system.

Keywords: base isolation; force reduction factor; damping; seismic analysis

1. Introduction

The seismic isolation system has been widely applied in the world to mitigate the damage risk of structures. It increases the range of flexibility of the structure base causing a period shift; and in turn, a considerable reduction in the elastic forces (Naeim and Kelly 1999). In addition, the energy dissipation due to the isolation system hysteretic behavior and the associated supplemental damping (damping ratio greater than 5%) affords further reduction in the forces. It is worth noting that at the range of medium to long periods of vibration (1.5 to 3.0 Sec.), the elastic responses of non-isolated and isolated structures are almost equal (Palazzo and Petti 1996, Naeim and Kelly 1999). This indicates that the base-isolated superstructures need little or no ductility demand.

The force reduction factor of base-isolated structures has been specified in different seismic design codes: UBC-97, IBC-2009, FEMA-356, and European code EC8, to be in the range of 1.5

*Corresponding author, Associate Professor, E-mail: serror@eng.cu.edu.eg
[a]Graduate Student
[b]Professor

 ISSN: 2092-7614 (Print), 2092-7622 (Online)

to 2.0, for the common lateral load resisting systems, which is much less than that of non-isolated structures. This is attributed to the aforementioned insignificant ductility demand of the isolated superstructure.

Although maximum displacement demand of seismic isolation systems can be obtained through nonlinear time history analysis, many approximate methods are frequently recommended in design codes and structural specifications to reduce the required computational effort and to simplify the design procedure (Tobia *et al*. 2014). One of the well-known methods is the equivalent linear method, in which the nonlinear response of the isolator can be adequately modeled using a viscously damped elastic structure.

In UBC-97, two procedures are defined for analysis of base-isolated structures, namely: the dynamic analysis and the simplified analysis. The dynamic analysis is applicable to any base-isolated structure and should be conducted in the form of a response spectrum analysis or a time history analysis. The simplified analysis is applicable with limitations (as per UBC-97, section 1657.5); meanwhile, it imposes a complicated formulation with sequence of tables and formulas. Step-by-step analysis procedure for base-isolated structures using UBC-97 has been documented by Naeim and Kelly (1999), Lee *et al*. (2001).

EC8 considered only the full isolation case, which means that the superstructure above the isolation system remains elastic and no need for capacity design and ductile detailing in the superstructure. Consequently, the elastic response spectrum is used in the design process after applying a modification due to the supplemental damping. EC8 indicated two simplified procedures: equivalent linear analysis and simplified linear analysis. The simplified procedures are not applicable to isolation systems with an effective damping ratio greater than 30%; in addition, the effective stiffness and damping are coupled forcing the code procedure to be complicated.

Murat and Srikanth (2007) evaluated the equivalent linear analysis procedure used in the design of seismic base-isolated structures. The effect of the intensity and frequency characteristics of the ground motion, isolator properties and the structure mass was considered in the evaluation. It has been reported that the effective damping equation currently used in the design of base-isolated structures must incorporate the effective period of the structure and frequency characteristics of the ground motion for more accurate estimation of seismic response. A further insight into the importance of the effective period has been reported by Nicos and Georgios (2013).

Ma *et al*. (2011) investigated the stochastic seismic response of a base-isolated high-rise building subjected to random earthquake ground motion. The equivalent linear analysis method was adopted using MDOF system for the superstructure, where the stochastic seismic response of the simplified system was obtained conveniently.

Leblouba (2012) presented a response spectrum analysis procedure suitable for base-isolated regular buildings subjected to near fault ground motions. The procedure was shown to be accurate enough for the preliminary design.

Varnavas and Petros (2013) evaluated the appropriateness of the linear and nonlinear models that can be used in the analysis of typical low-rise base-isolated steel buildings, taking into account the inherent nonlinearities of the isolation system as well as the potential nonlinearities of the superstructure in case of strong ground motions. The accuracy of the linearization was evaluated comparatively with the corresponding response that can be obtained through the nonlinear time history analysis. Furthermore, the common assumption of elastic behavior for the superstructure was validated.

Tao *et al*. (2014a, 2014b), Tobia *et al*. (2014) assessed different equivalent linear methods proposed in the literature based on SDOF systems with bilinear hysteretic behavior. Numerical

simulations were performed including both approximate linear and exact nonlinear analyses. The results revealed that an improvement in the prediction accuracy of the equivalent linear analysis can be achieved through introducing a factor which is related to ductility ratio, post-yield to elastic stiffness ratio and initial period of isolation system.

Chao *et al*. (2014) proposed a computational method for system identification for obtaining insight into the linear and nonlinear structural properties of based-isolated buildings. A bilinear hysteresis model was adopted for the isolation system and the superstructure was assumed linear.

In this study, a simplified seismic analysis procedure has been proposed based on the well documented N2 method (Fajfar and Eeri 2000) which empowers the proposed procedure through its direct and friendly formulations; meanwhile, its application to seismic analysis of base-isolated structures has been discussed and validated by Kilar and Koren (2008, 2009). The damping modification factors have been discussed in order to modify the N2 method to account for the supplemental damping effect. Hence, a comprehensive analysis has been performed for base-isolated structure models for direct application and verification of the proposed procedure. In addition, a discussion has been elaborated for the results with respect to the dynamic characteristics of the base isolation system.

2. Damping modification factor

It is fact that pseudo velocity and pseudo acceleration used in the seismic design codes differ greatly from the actual velocity and acceleration in case of damping ratios greater than 5% (Sadek *et al*. 2000). Accordingly, damping modification factor is typically required for the design and analysis of a typical structure equipped with supplemental damping devices to approximately estimate its elastic response from its counterpart at 5% damping. Extensive research works have been conducted to investigate and assess the damping modification factors for displacement, velocity and acceleration (Newmark and Hall 1982, Kawashima and Aizawa 1986, Ashour and Hanson 1987, Wu and Hanson 1989, Tolis and Faccioli 1999, Bommer *et al*. 2000, Sadek *et al*. 2000, Ramirez *et al*. 2002, Lin and Chang 2003, Priestley and Grant 2005, Bommer and Mendis 2005, Takewaki 2009, Hatzigeorgiou 2010). In this study, eight methods that have well contributed to the design codes have been introduced and discussed.

Newmark and Hall (1982) presented the earliest method, where the data were limited to a maximum viscous damping ratio of 20%. It was implemented in ATC-40 and FEMA-273 for the displacement-based evaluation design of existing buildings, and in UBC-97, NEHRP-97, FEMA-356 and IBC-2000 for the design of buildings with seismic isolation systems and passive energy dissipation systems. The damping modification factor is expressed in terms of viscous damping ratio (ξ) and vibration period (T) as B=[1.514−0.321ln(ξ)] for constant acceleration region B=[1.4−0.248ln(ξ)] for constant velocity region and B=[1.309−0.194ln(ξ)] for constant displacement region.

Ashour and Hanson (1987) studied the effect of supplemental damping on the earthquake spectral displacement, where the data were derived for viscous damping ratios up to 150% and vibration periods up to 3.0 seconds. Ashour and Hanson method was implemented in UBC-94 and NEHRP-94 for the design of buildings with passive energy dissipation systems. The damping modification factor is expressed in terms of viscous damping ratio (ξ) as $B=[0.05(1-e^{-\alpha a\xi})/\xi(1-e^{-0.05\alpha a})]^{0.5}$, where α_a is a numerical coefficient that is set to 18 and 65 for the upper and low bound of B, respectively, and it is adopted by NEHRP-94 as 18.

Wu and Hanson (1989) presented the damping modification factor using damping ratios between 10% and 50% and vibration periods up to 10.0 seconds. Two periods in the constant acceleration region, one in the constant velocity region and two in the constant displacement region were selected. Accordingly, the damping modification factor is expressed in terms of viscous damping ratio (ξ) and vibration period (T) as $B=[\psi(\xi,T)/\psi(\xi=5\%,T)]$, where $\psi=[-0.349\ln(0.0959\xi)]$ for $T=0.1$ Sec. $\psi=[-0.547\ln(0.417\xi)]$ for $T=0.5$ Sec. $\psi=[-0.471\ln(0.524\xi)]$ for $0.5<T<3.0$ Sec. $\psi=[-0.478\ln(0.475\xi)]$ for $T=3.0$ Sec. and $\psi=[-0.291\ln(0.0473\xi)]$ for $T=10.0$ Sec. The linear interpolation is applied in the period range from 0.1 Sec. to 0.5 Sec. and in the range from 3.0 Sec. to 10.0 Sec.

Bommer *et al.* (2000) developed a simple procedure to construct displacement response spectra for the damped system, where the data were derived for viscous damping ratios up to 30% and vibration periods up to 3.0 Sec. The damping modification factor is expressed in terms of viscous damping ratio (ξ) as $B=[10/(5+\xi)]^{0.5}$.

Sadek *et al*. (2000) established three distinct damping modification factors for displacement, velocity and acceleration responses, where the data were derived for viscous damping ratios up to 60% and vibration periods up to 4.0 Sec. The displacement modification factor (B_d) is given in a table form in terms of viscous damping ratio (ξ) and vibration period (T). Meanwhile, the acceleration modification factor (B_a) is expressed as $B_a=B_d(1+a_aT^{ba})$, where $a_a=(2.436\xi^{1.895})$, and $b_a=(0.628+0.205\xi)$.

Ramirez *et al*. (2002) method was employed in NEHRP-2000 for the design of building with supplemental damping systems, where the data were derived for viscous damping ratios up to 100% and vibration periods up to 4.0 Sec. The damping modification factor is expressed in terms of viscous damping ratio (ξ) and vibration period (T) as $[B=B_s]$ for $T=0.2T_s$ and $[B=B_l]$ for $T\geq T_s$. For $0.2T_s<T<T_s$, B is determined by linear interpolation between B_s and B_l. For $T<0.2T_s$, B is determined by linear interpolation between 1.0 and B_s. T_s is the period at intersection between the constant velocity and constant acceleration regions. B_s and B_1 are damping coefficients given by Ramirez et al. in a table form in terms of (ξ).

Lin and Chang (2003) proposed a period-dependent formula, where the data were derived for viscous damping ratios up to 50% and periods from 0.01 to 10.0 seconds. The damping modification factor is expressed in terms of viscous damping ratio (ξ) and vibration period (T) as $B=[1-(aT^{0.3}/(T+1)^{0.65}]$, where $[a=1.303+0.436\ln(\xi)]$.

Hatzigeorgiou (2010) proposed empirical expressions to estimate the damping modification factors for displacement, velocity and acceleration responses, where the data were derived for viscous damping ratio in the range from 0.5% to 50%, and vibration periods from 0.1 to 5.0 seconds. Three different strong ground motion databases were examined with a total of 310 records including far-fault, near-fault and artificial earthquakes in association with different soil conditions from hard rock to soft soil. The damping modification factor is expressed in terms of viscous damping ratio (ξ), vibration period (T), and numerical phenomenological coefficients which enable the same formula to be employed for displacement, velocity and acceleration modification: $B=1+[(\xi-5)\times(1+C_1\ln(\xi)+C_2(\ln(\xi))^2)\times(C_3+C_4\ln(T)+C_5(\ln(T))^2)]$, where $C_i(i=1-5)$ are numerical phenomenological coefficients in Tables form.

It is challenging to choose among the introduced eight methods for damping modification factor. Fig. 1 reports the following comparative observations for the displacement damping modification factor (DDMF):

- The higher the viscous damping ratios are, the smaller the damping modification factors become.

- In the short period range (as example T=0.5 Sec.), the modification factor proposed by Newmark and Hall is smaller than that proposed by the other methods. In an ascending order: Newmark and Hall is followed by Hatzigeorgiou, Sadek *et al*., Lin and Chang, Bommer *et al*., Ashour and Hanson, Wu and Hanson, Ramirez *et al*.. This means that the smallest response will be predicted by Newmark and Hall method while the largest response will be predicted by Ramirez *et al*., in the short period range.

- In the long period range (as example T=3.0 Sec.), the modification factor proposed by Wu and Hanson is smaller than that proposed by the other methods. In an ascending order: Wu and Hanson is followed by Bommer *et al*., Ashour and Hanson, Lin and Chang, Sadek *et al*., Ramirez *et al*., Hatzigeorgiou and Newmark and Hall. This means that the smallest response will be predicted by Wu and Hanson method while the largest response will be predicted by Newmark and Hall, in the long period range.

- In the short period range, the modification factors proposed by Bommer *et al*., Ashour and Hanson, and Wu and Hanson are almost identical. On the other hand, at the long period range, the modification factors given by Bommer *et al*. and Ashour and Hanson are very close to each other.

- In the long period range and for damping ratios from 20% to 50%, Hatzigeorgiou method gives values greater than the other methods.

- It is worth noting that all methods appear to have a consistent pattern for the DDMF which is attributed to the fact that they are all formulated based on the spectral displacement. This is not the case for the acceleration damping modification factor (ADMF), as discussed hereafter, where the methods are based on the pseudo acceleration except that of Hatzigeorgiou (2010).

- It is evident that the damping modification factor has a range of 1.25 to 2.5 for a damping ratio in a range of 10% to 50%. This is consistent with the range specified in different seismic design codes (UBC-97, IBC-2009, FEMA-356 and EC8) in between 1.5 to 2.0 for the most common lateral load resisting systems of base-isolated structures.

The damping modification factors proposed by: Newmark and Hall, Wu and Hanson, Lin and Chang, Hatzigeorgiou, Sadek *et al*., Ramirez *et al*. are period-dependent, while the damping modification factors proposed by Ashour and Hanson, Bommer *et al*. are period independent. In addition, only Hatzigeorgiou, Sadek *et al*., Lin and Chang have the vibration period as direct input in their formula. Moreover, only Hatzigeorgiou, Sadek *et al*. have ADMF in addition to the DDMF. It has been reported that the damping modification factors are strongly dependent on the period of vibration (Hatzigeorgiou 2010). Furthermore, considering that the majority of existing codes are traditionally based on the seismic forces evaluation, the ADMF should be in concern. Accordingly, a further comparison has been conducted for only three methods: Hatzigeorgiou, Sadek *et al*., Lin and Chang. For these three methods, Figs. 2 and 3 illustrate the relationship between the damping modification factors and the period of vibration for viscous damping ratios equal to 10%, 30%, and 50%.

Fig. 2 is for the displacement damping modification factor (DDMF). It is evident that as the damping ratio increases the difference between the three methods increases; however, the values proposed by Sadek et al., and Lin and Chang are very close to each other while those proposed by Hatzigeorgiou differ from them in the long period range and at the damping ratios 20% and 30%. This is attributed to the higher DDMF proposed by Hatzigeorgiou method in this range as reported in Fig. 1. Fig. 3 is for the acceleration damping modification factor (ADMF). It is evident that the values of Lin and Chang differ strongly from those of Hatzigeorgiou, Sadek *et al*. This is attributed to the fact that Lin and Chang adopted only one modification factor based on the displacement response; meanwhile, Hatzigeorgiou, Sadek *et al*. adopted two distinct factors for both acceleration

and displacement. It is evident also that the results from Sadek *et al.* show disturbances at different damping ratios, while Hatzigeorgiou results show consistent pattern. This can be attributed to the formulation of Sadek *et al.* method that is based on pseudo acceleration rather than actual acceleration.

It is worth noting that any of the discussed methods can be employed in the proposed procedure for damping modification. Meanwhile, in this study the authors adopted Hatzigeorgiou method, considering that it has been formulated based on: the direct input of vibration period; and the actual acceleration rather than the pseudo acceleration.

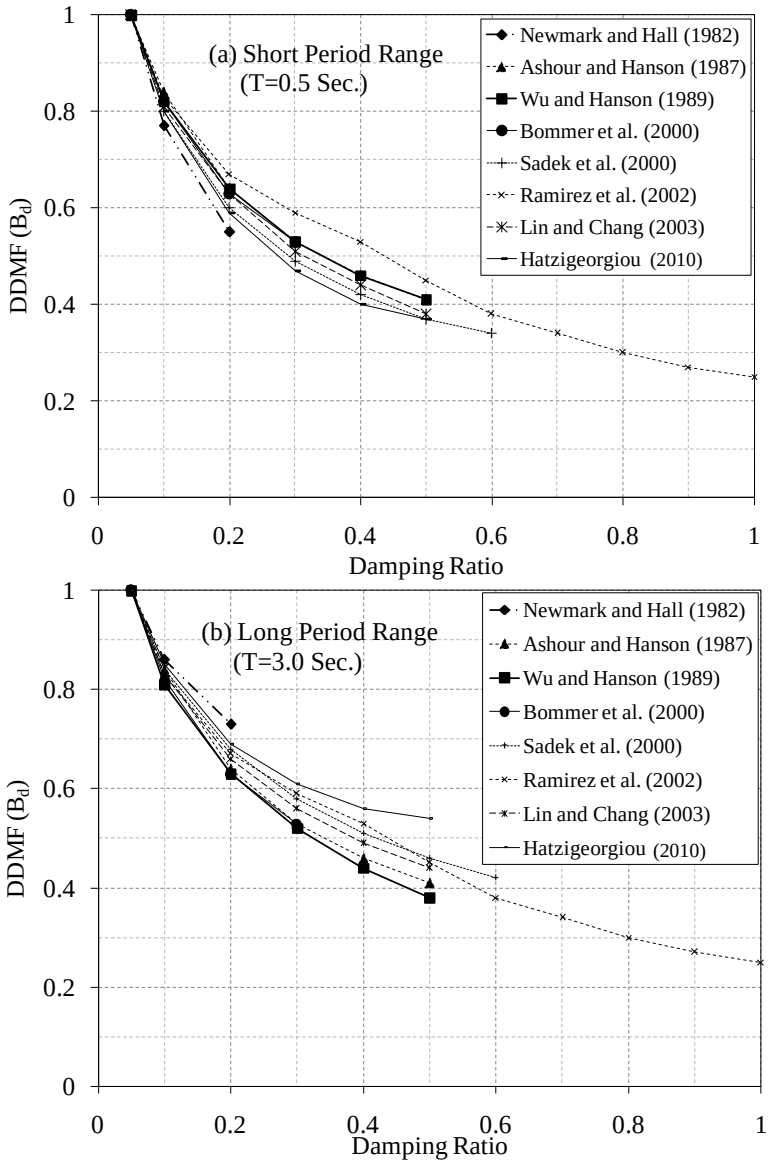

Fig. 1 Displacement Damping Modification Factor (B_d) versus damping ratio at: (a) short period range (T=0.5 Sec.), and (b) long period range (T=3.0 Sec.)

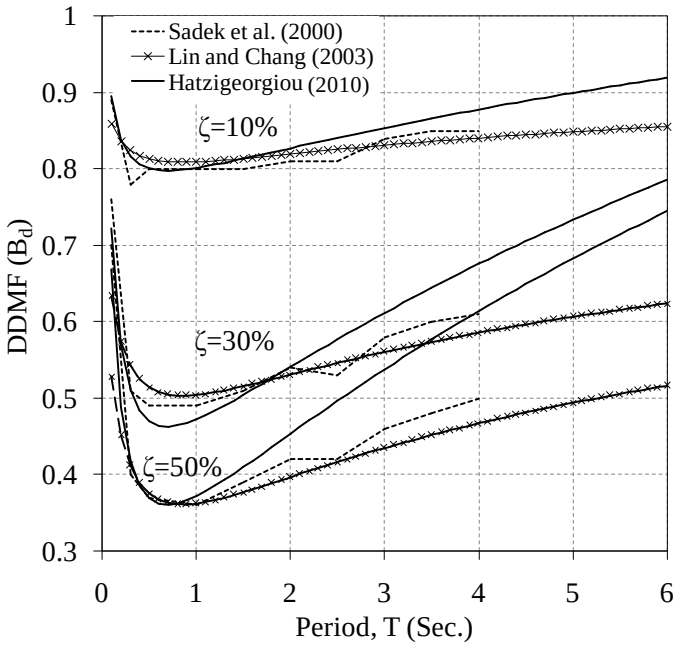

Fig. 2 Displacement Damping Modification Factor (B_d) versus periods of vibration for different damping ratios

3. Proposed seismic analysis procedure

The proposed seismic analysis procedure has been derived based on three basic assumptions which set the procedure limitations. The first assumption is that for a base-isolated structure the displacement is concentrated at the isolation level; therefore, the superstructure moves almost as a rigid body representing a single mode of vibration. The second assumption is that the effective damping of the isolation system is considered instead of the average damping value for the whole structure system. This is attributed to the rigid body response of the superstructure as indicated in the first assumption. The third assumption is that the superstructure is considered to remain elastic. It is worth noting that the aforementioned assumptions have been adopted in order to enhance the procedure simplicity without loss of accuracy, since these assumptions are typical for most of the simplified methods in different seismic design codes (Kilar and Koren 2009, Tobia *et al*. 2014).

Hereafter, the proposed procedure steps, verification and discussion have been presented; meanwhile, further details have been given in the reference (El-Gazzar 2013).

3.1 Procedure steps

Fig. 4 illustrates the steps of the proposed seismic analysis procedure which can be summarized as follows:

Step-1: Establish demand spectrum

Starting from an elastic demand spectrum with desired peak ground acceleration and local soil condition, the displacement can be obtained for an elastic SDOF system. This is normally applied to vibration periods up to 4.0 Sec. However, for base-isolated structures, longer vibration periods

may be attained; consequently, the elastic spectral displacement is obtained as discussed by Bommer and Mendis (2005).

The inelastic demand spectrum is obtained by taking into account the force reduction factor (R) that represents the nonlinear behavior of the superstructure. For the N2 method, the ductility reduction factor (R_μ) is considered (Fajfar and Eeri 2000). Meanwhile, it has been reported that the equal displacement rule of the N2 method can still be applied to structural systems with a positive post-yield stiffness and higher damping (Kilar and Koren 2009). Accordingly, Fig. 5 illustrates the relation between the ductility reduction factor in case of positive post-yield stiffness (R_α) and the ductility reduction factor in case of zero post-yield stiffness (R_μ). This can be expresses as $R_\alpha=R_\mu/(\alpha R_\mu-\alpha+1)$, where α is the ratio between the post-yield stiffness K_p to the elastic stiffness K_e of the system. The inelastic acceleration ordinate of the demand spectra can then be obtained by dividing the elastic acceleration demand by R_α; meanwhile, the inelastic displacement equals the elastic one based on the equal displacement rule. It is worth noting that based on the assumption of

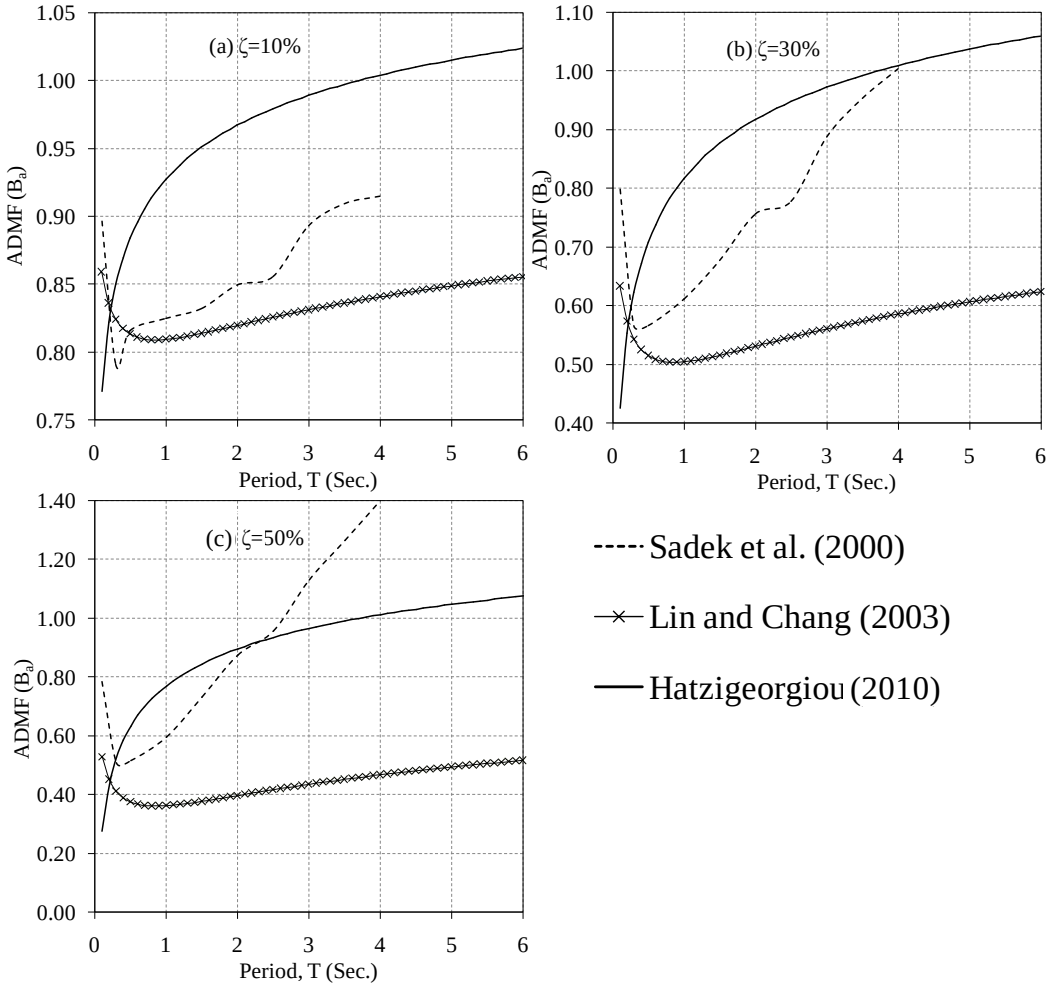

Fig. 3 Acceleration Damping Modification Factor (B_a) versus periods of vibration for different damping ratios: (a) 10%, (b) 30%, and (c) 50%

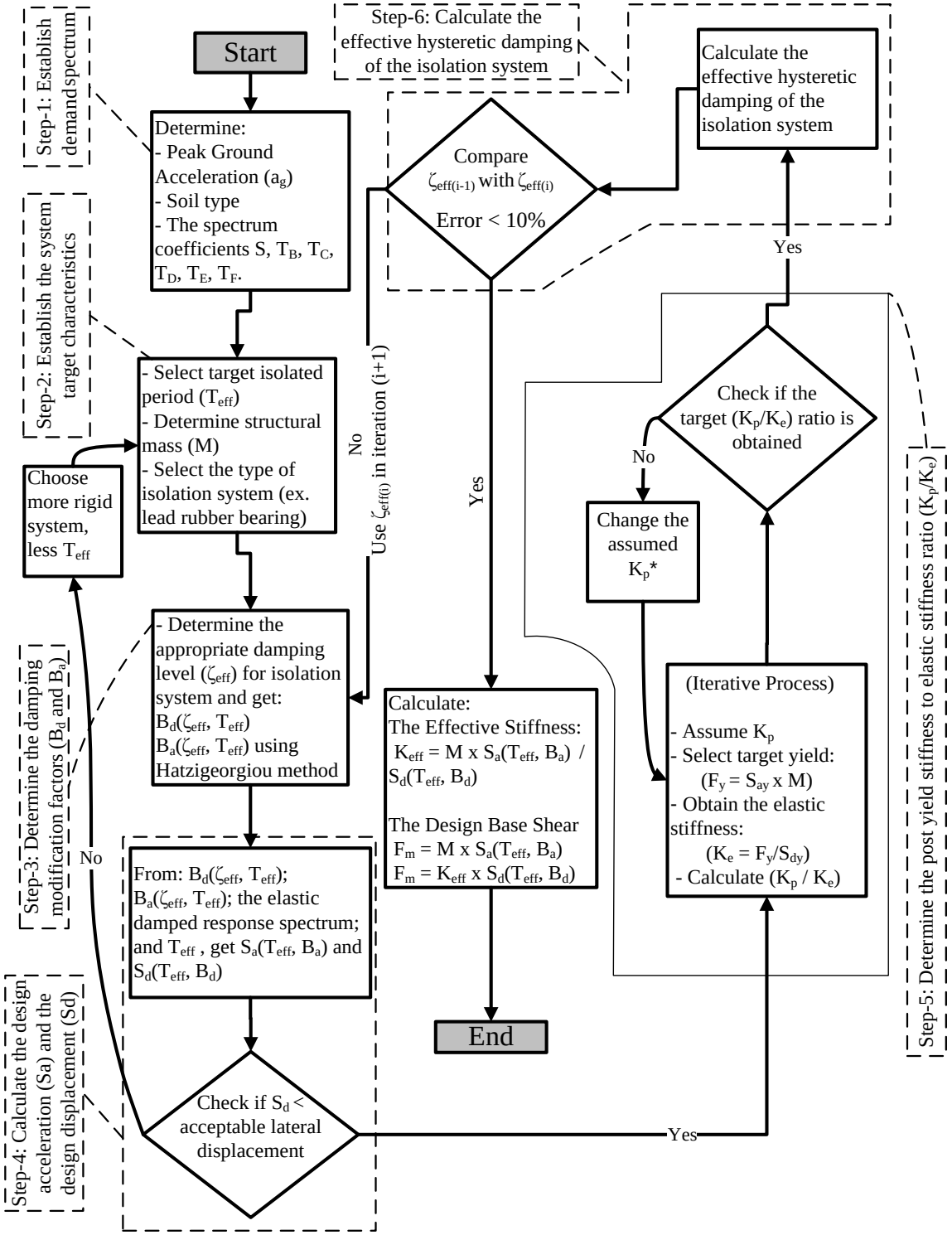

Fig. 4 Proposed procedure steps

elastic superstructure the ductility reduction factor R_α equals 1.0. In other words, the inelastic spectrum is identical to the elastic one.

The damped elastic demand spectrum is then obtained by scaling both the acceleration ordinate and the displacement ordinate of the elastic demand spectrum with the appropriate damping modification factors as determined in Step-3.

Step-2: Establish the system target characteristics

As a result of the rigid body assumption, the base displacement is obtained instead of the top displacement. Consequently, the dynamic characteristics that represent the hysteretic behavior of the bilinear system are: the effective period (T_{eff}), the total mass (M), the yield strength (S_{ay}, or $F_y=M\times S_{ay}$), the target ratio of post yield stiffness to the elastic stiffness ($\alpha=K_p/K_e$) and the effective damping (ξ_{eff}). It is worth noting that the K_p/K_e ratio and the effective damping (ξ_{eff}) are initially set to target values.

Step-3: Determine the damping modification factors (B_d and B_a)

Since the superstructure and the base isolation system have different damping characteristics, an average damping value should be considered for the whole system. However, for the assumption that the superstructure moves almost as a rigid body, the damping modification factor will be obtained using the effective damping of the isolation system (Kilar and Koren 2008). Hence, the damped elastic demand spectrum is then obtained by scaling both the acceleration ordinate and the displacement ordinate of the elastic demand spectrum (obtained in Step-1) with the displacement damping modification factor (B_d) and the acceleration damping modification factor (B_a), respectively. The factors of Hatzigeorgiou (2010) have been employed using the effective damping of the isolation system.

Step 4: Obtain the design acceleration (S_a) and the design displacement (S_d)

Based on steps 1-3 and as illustrated in Fig. 6, the design force of the system (F_m) equals the damped design acceleration (S_a) times the system mass (M), and the design displacement (S_d) is obtained at the intersection between the capacity curve (the effective stiffness line, K_{eff}) and the damped elastic demand spectrum curve. The effective stiffness is calculated as $K_{eff}=M\times S_a(T_{eff},B_a)/S_d(T_{eff},B_d)$.

Step-5: Determine the post-yield stiffness to elastic stiffness ratio (K_p/K_e):

In order to determine the post-yield stiffness (K_p) and the elastic stiffness (K_e) an iterative process is required as follows:

a. The post-yield stiffness is assumed with a value bounded within the hatched area in Fig. 6.

b. The yield displacement is obtained at the intersection point between the post-yield stiffness line and the horizontal line associated with the yield point (S_{ay}), see Fig. 6.

c. The elastic stiffness is then obtained as: $K_e=F_y/S_{dy}$, where F_y is the yield strength of the system, and S_{dy} is the associated yield displacement.

d. The ratio of the post-yield stiffness to the elastic stiffness is then calculated and checked against the target ratio.

The iterative process continues from (a) to (d) till convergence to the target K_p/K_e ratio.

Step-6: Determine the Effective Damping of the Isolation System (ξ_{eff}):

The effective hysteretic damping of the isolation system is calculated as $\xi_{eff}=A_h/\left(2\pi K_{eff}S_d^2\right)$, where, A_h is the area of the hysteresis loop (the energy dissipated per cycle) as shown in Fig. 7. It is worth noting that the calculated parameters: K_{eff}, K_p, K_e, S_{ay}, and S_d, will yield a different effective damping compared with the one initially targeted in Step 2. Consequently, an iterative process is required till convergence to the target damping ratio.

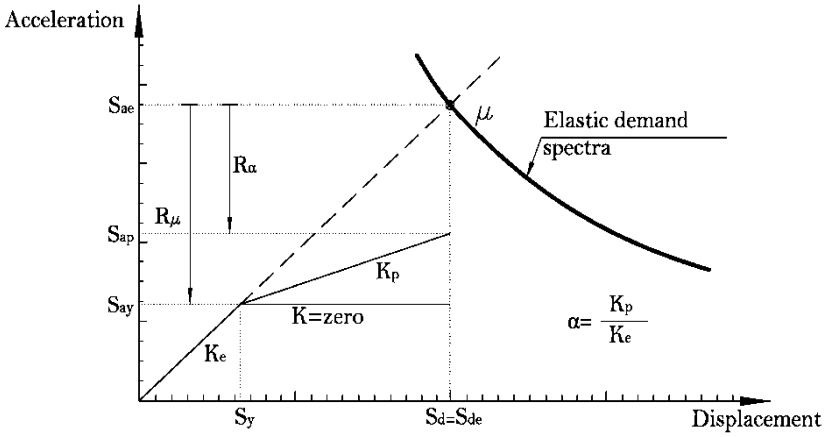

Fig. 5 Relation between R_α and R_μ by applying the equal displacement rule

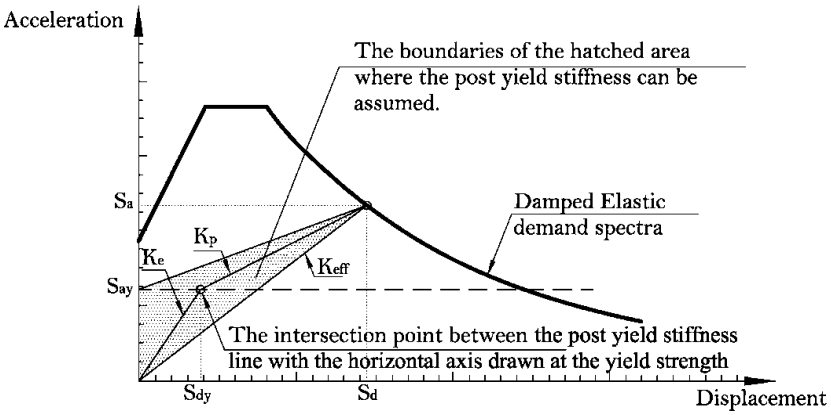

Fig. 6 Representation of seismic demand of base-isolated structure

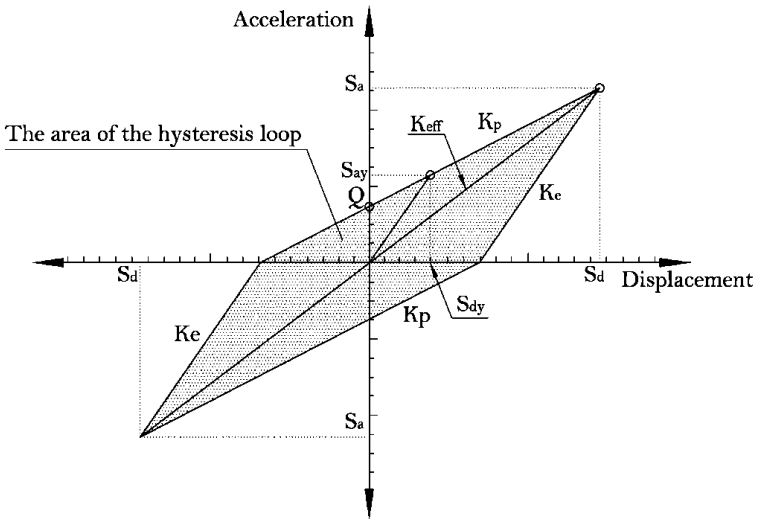

Fig. 7 Representation of the effective hysteretic damping of the base isolation system

3.2 Procedure application and verification

In this section, seismic analysis has been performed for base-isolated steel moment resisting frames using the proposed procedure. Different parameters have been examined including: post-yield stiffness to elastic stiffness ratio (K_p/K_e); effective stiffness (K_{eff}); effective damping (ξ_{eff}); effective period (T_{eff}) and yielding strength (F_y), using lead rubber bearing as sample base isolation system. The analysis results have been verified against those of EC8 and the nonlinear time history analysis. In addition, the proposed procedure has been verified against numerical and experimental investigations in the literature.

3.2.1 Modeling and analysis

Fig. 8(a) shows a steel moment resisting frame with lead rubber bearing (LRB) isolation system. The steel frame has been modeled as a SDOF system where the lumped mass has been calculated in accordance with the shown distributed loads.

For design and analysis purpose, the hysteresis loop is usually represented as a bilinear curve that describes the isolation model characteristics. The lead rubber bearing isolation system has been characterized by a bilinear spring model as shown in Fig. 8(b). The model is represented by: elastic stiffness (unloading stiffness), post yield stiffness, effective stiffness, characteristic strength, yield strength, effective damping, maximum displacement, and yield displacement.

It has been reported that the elastic stiffness ranges between 6.5 to 25 times the post-yield stiffness (Kelly 2001). In this study, K_p/K_e ratio is taken as 4%, 7%, 10%, 13% and 15%. On the other hand, the effective stiffness K_{eff} is defined as the secant slope of the peak-to-peak values in a hysteresis loop (Naeim and Kelly 1999), and it has been calculated as $K_{eff}=M(2\pi/T_{eff})^2$, where ($M$) is the total mass of the isolated structure and (T_{eff}) is the target effective period. It should be noted that the target effective period is the period of the isolation system assuming that the superstructure is rigid. Different values for the yield strength (F_y) have been considered as: 14 kN, 27.8 kN, 41.7 kN, and 55.6 kN.

Using simple geometric relations in Fig. 8(b), the yield strength and the yield displacement can be expressed, respectively, as $F_y=Q+(S_{dy}K_p)$ and $S_{dy}=Q/(K_e-K_P)$. The base shear (design force) at particular displacement (design displacement) can, in turn, be expressed (Kelly 2001) as $F_m=Q+(S_dK_P)=K_{eff}S_d=S_a(T_{eff})M$. The effective damping ξ_{eff} has been calculated based on the formula $\xi_{eff}=A_h/(2\pi K_{eff}S_d^2)$, where, $A_h=4Q(S_d-S_{dy})$. Q is the characteristic shear strength of the lead rubber bearing.

Type-I response spectrum, in accordance with the European code EC8, has been employed with a peak ground acceleration of 0.30 g, and local soil of type-B. The characteristic vibration periods have been considered as follows: T_B=0.15 Sec., T_C=0.5 Sec. and T_D=2.0 Sec. The damping modification factors of Hatzigeorgiou (2010) have been employed based on the effective damping of the isolation system.

For the time history analysis, the REXEL software (Iervolino *et al*. 2010) has been used to select an ensemble of seven earthquake ground motion records. The software enables that the average spectrum of the seven records be in compliance with the employed EC8 response spectrum. As being evident in Fig. 9, the average spectrum varies from the target EC8 spectrum with upper and lower tolerances of ±10%, which is an accepted selection. According to EC8, using seven ground motion records for time history analysis is sufficient to consider the average response of the parameter in question. The characteristics of the selected ground motion records have been listed in Table 1.

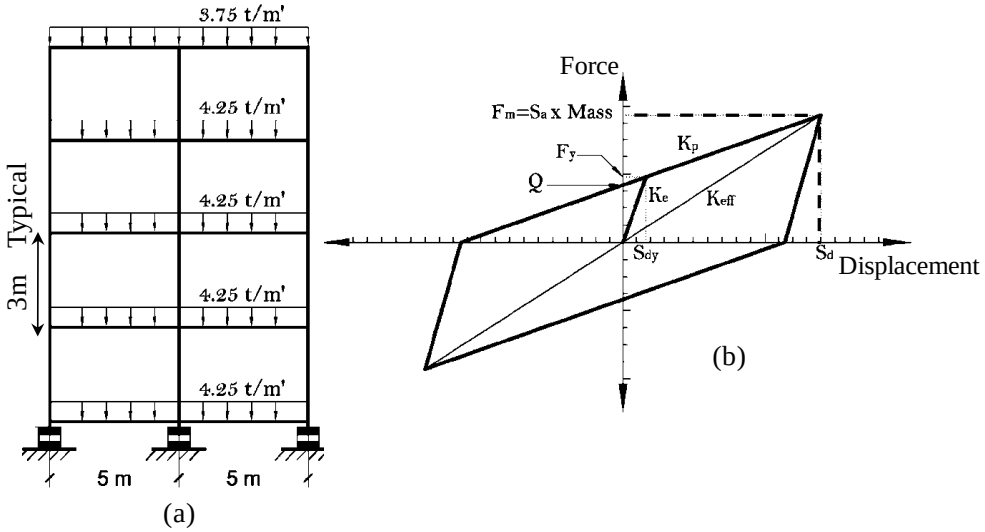

Fig. 8 Steel moment resisting frame with LRB isolation system: (a) Typical frame elevation and mass, and (b) LRB idealized hysteresis loop

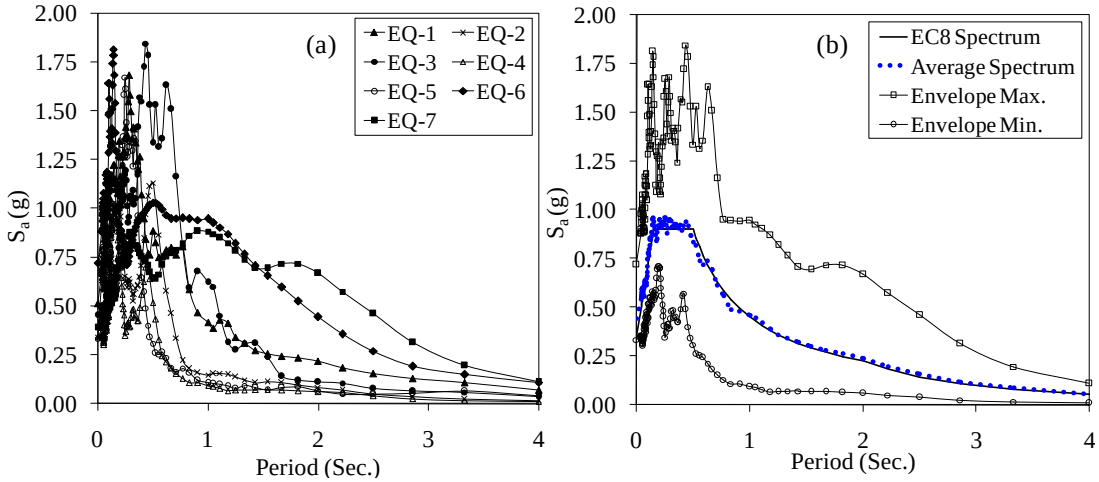

Fig. 9 (a) Response spectrum of the selected ground motion records; and (b) EC8 Spectrum versus the average, maximum and minimum spectrum of the selected ground motion records

Table 1 Characteristics of the selected ground motion records

Earthquake	Station	Magnitude	Direction
EQ-1: South Iceland	ST2484	6.5	Y-component
EQ-2: Friuli (aftershock)	ST24	6.0	Y-component
EQ-3: Montenegro	ST62	6.9	X-component
EQ-4: Friuli (aftershock)	ST24	6.0	X-component
EQ-5: South Iceland (aftershock)	ST2484	6.4	X-component
EQ-6: South Iceland (aftershock)	ST2488	6.4	Y-component
EQ-7: Erzincan	ST205	6.6	X-component

3.2.2 Results and discussion

Fig. 10 illustrates the effect of the isolation system parameters on the effective stiffness (K_{eff}). It is evident that the K_p/K_e ratio has no effect on the effective stiffness. This observation is apparent in Fig. 7 where the slope of the line extending from the origin point up to the (S_d, S_a) point is representing the effective stiffness and is independent of the K_p/K_e ratio. The yield level of the isolation system (F_y), however, affects the effective stiffness, where it increases as the yield level increases. With increasing the yield level from 14 kN to 55.6 kN, the effective stiffness increases with a percentage of 23% and 40%, at the effective periods of 1.6 Sec. and 3.0 Sec. respectively. The pattern of variation for the effective stiffness versus the effective period is consistent with the literature (Lin *et al*. 2005), where the effective stiffness decreases as the effective period increases.

Fig. 11 illustrates the effect of the isolation system parameters on the effective damping (ξ_{eff}). It is evident that the K_p/K_e ratio has insignificant effect on the effective damping. Meanwhile, increasing the K_p/K_e ratio decreases the effective damping due to the shrinkage of the hysteresis

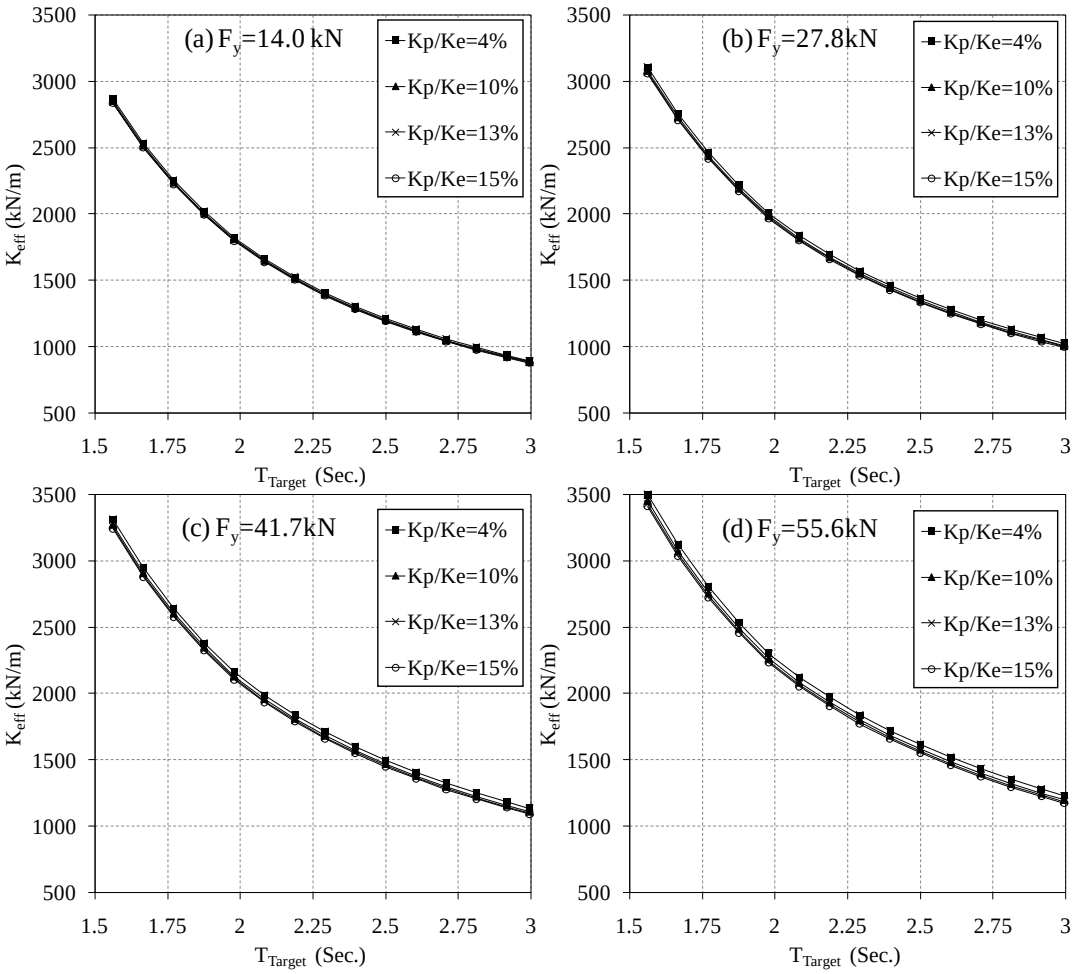

Fig. 10 The effective stiffness versus the target effective period of vibration at different K_p/K_e ratios and for: (a) F_y=14 kN; (b) F_y=27.8 kN; (c) F_y=41.7 kN; and (d) F_y=55.6 kN

loop. With increasing the K_p/K_e ratio from 4% to 15%, the effective damping decreases with a percentage of 5% and 12%, at the effective periods of 1.6 Sec. and 3.0 Sec. respectively, for a yield level of 14 kN. On the other hand, with increasing the K_p/K_e ratio from 4% to 15%, the effective damping decreases with a percentage of 16% and 20%, at the effective periods of 1.6 Sec. and 3.0 Sec. respectively, for a yield level of 55.6 kN. It is also evident that the yield level of the isolation system (F_y) affects significantly the effective damping, where it increases as the yield level increases due to the expansion of the hysteresis loop. With increasing the yield level from 14 kN to 55.6 kN, the effective damping increases with a percentage of 400% and 300%, at the effective periods of 1.6 Sec. and 3.0 Sec. respectively. The pattern of variation for the effective damping versus the effective period is consistent with the literature (Lin *et al*. 2005), where the effective damping increases as the effective period increases.

Figs. 12 and 13 illustrate the effect of the isolation system parameters on both the design force (F_m) and the design displacement (S_d), respectively. It is evident that the K_p/K_e ratio has negligible

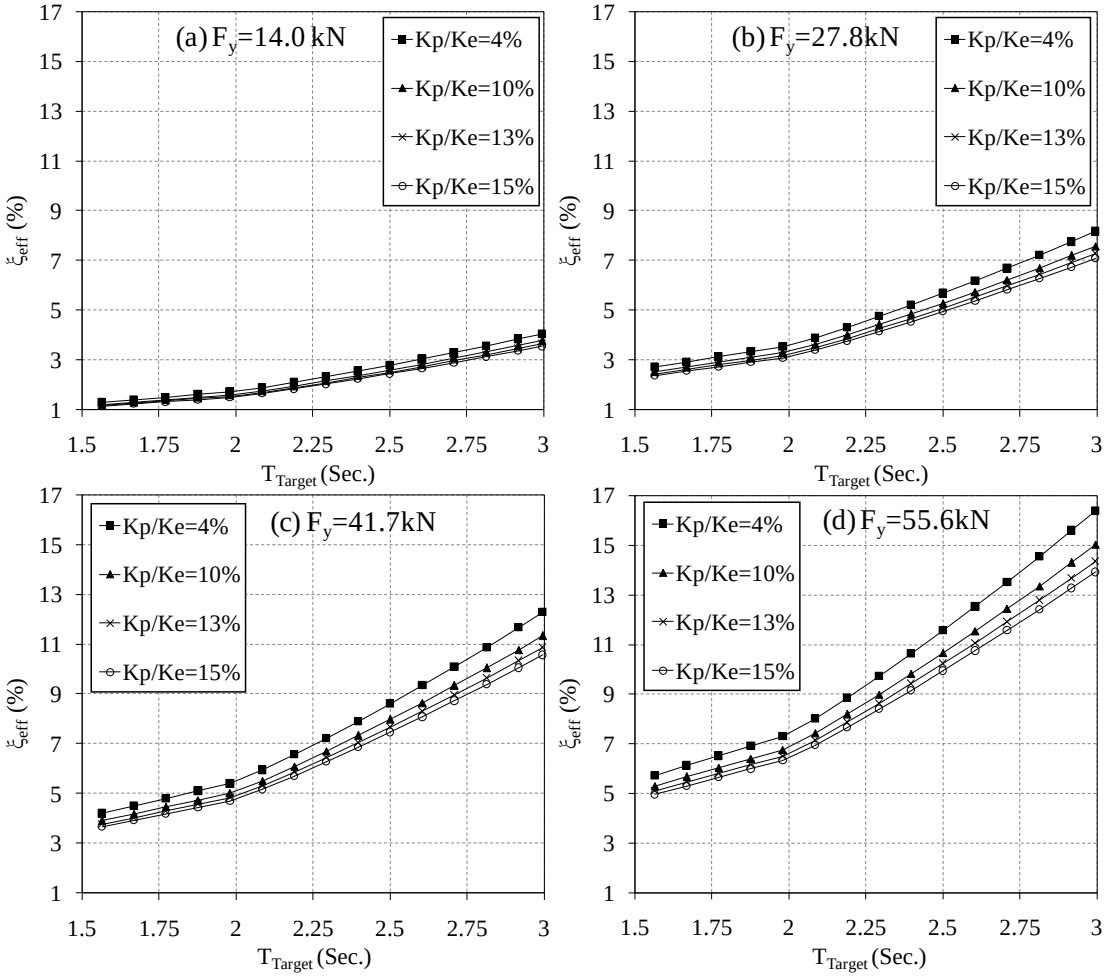

Fig. 11 The effective damping ratio versus the target effective period of vibration at different K_p/K_e ratios and for: (a) F_y=14 kN; (b) F_y=27.8 kN; (c) F_y=41.7 kN; and (d) F_y=55.6 kN

effect on both the design force and the design displacement. This is attributed to the negligible effect of the K_p/K_e ratio on both the effective stiffness and the effective damping of the system as reported in Figs. 10 and 11, respectively. The yield level of the isolation system (F_y), apparently, affects the induced design force and displacement. It is evident that the design force and displacement decrease as the yield level increases. This is attributed to the significant reduction in the demand spectrum due to the increase in the effective damping, compared with the increase in the effective stiffness. It is worth noting that the pattern of variation for the design force and the design displacement versus the effective period is consistent with both the acceleration and displacement response spectrum patters, respectively, and in agreement with the literature (Lin *et al*. 2005).

The results of the proposed procedure have been verified against those of the European code EC8 and the nonlinear time history analysis, as shown in Figs. 12 and 13 for the design force (F_m) and the design displacement (S_d), respectively, where the results are in good agreement. The maximum difference between the proposed procedure and the time history analysis can be quantified as 17% for both force and displacement results. Meanwhile, the maximum difference between EC8 and the time history analysis can be quantified as 22% for both force and

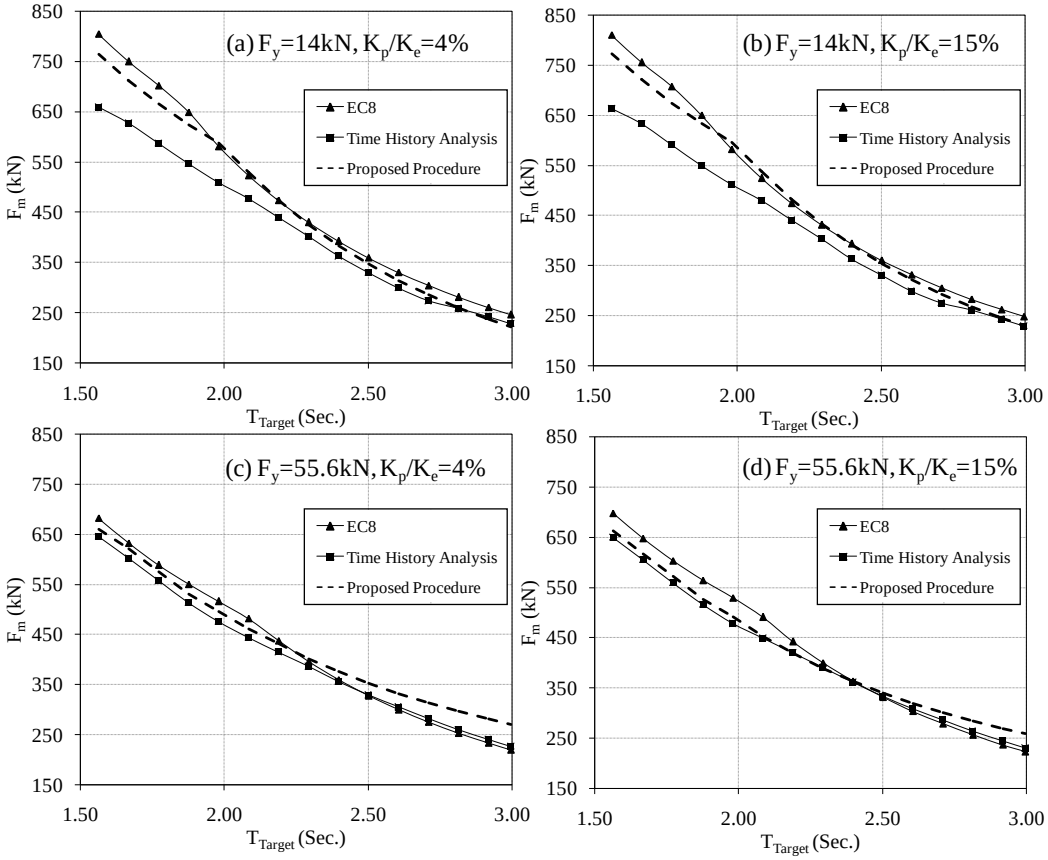

Fig. 12 The proposed procedure force verification against EC8 and time history analysis for: (a) F_y=14 kN, and K_p/K_e=4%; (b) F_y=14 kN, and K_p/K_e=15%; (c) F_y=55.6 kN, and K_p/K_e=4%; and (d) F_y=55.6 kN, and K_p/K_e=15%

displacement results. As shown in Fig. 12, the design force results are in better agreement with EC8 and the time history analysis at the yield level of 55.6 kN compared with those at the yield level of 14 kN. This is attributed to the resulted effective damping that is less than 5% at the low yield level and more than 5% (up to 20%) at the high yield level. In addition; the ADMF of Hatzigeorgiou method well contributed to force results through employing the actual acceleration rather than the pseudo one. Similarly, as shown in Fig. 13, the design displacement results are in better agreement with EC8 at the yield level of 55.6 kN compared with those at the yield level of 14 kN. This is attributed to the inadequacy of EC8 damping modification factor with the effective damping ratios less than 5% at the low yield level; in addition, the damping modification factor of EC8 is considered for the acceleration spectrum modification rather than the displacement spectrum (Bommer *et al*. 2000).

The results of the proposed procedure have been also verified against those of numerical and experimental investigations in the literature, as listed in Table 2. The proposed procedure revealed results that are in good agreement with those indicated in the numerical test of Kilar and Koren (2009) for a base-isolated reinforced concrete building. It is worth noting that the difference in the obtained force (around 23.69%) is attributed to the fact that Kilar and Koren considered the inelastic response of the superstructure and in turn the induced force reduction due to ductility; meanwhile, the proposed procedure assumes elastic superstructure. In addition, the proposed procedure revealed results that are in good agreement with those indicated in the experimental test of Xing *et al*. (2012) for a lead rubber bearing isolator. It is worth noting that the experimental

Table 2 Procedure verification against numerical and experimental results in literature

Base Isolation Characteristics		Published Work Results	Proposed Procedure Results	Error (%)
Kilar and Koren (2009): Numerical test for LRB:	Displacement (mm)	130	129.7	0.80
Elastomer height=150 mm Elastomer diameter=350 mm Lead core diameter=77 mm No. of isolators=24 Mass=124.77 Ton.Sec^2/m K_{eff}=958 kN/m per isolator K_p=650 kN/m per isolator K_p/K_e=15.38%	Force (kN)	130	160.8	23.69
	ξ_{eff} (%)	18.7	17.4	6.90
	T_{eff} (Sec.)	1.52	1.52	0.00
Xing *et al*. (2012): Experimental test for LRB:	Displacement (mm)	60	52.52	12.50
Elastomer height=106.5 mm Elastomer diameter=300 mm Lead core diameter=60 mm No. of isolators=1 Mass=3.5 Ton.Sec^2/m K_{eff}=826 kN/m K_p=457 kN/m K_p/K_e=10.0%	Force (kN)	48	43.27	9.85
	ξ_{eff} (%)	27.35	27.35	0.00
	T_{eff} (Sec.)	1.293	1.295	0.15

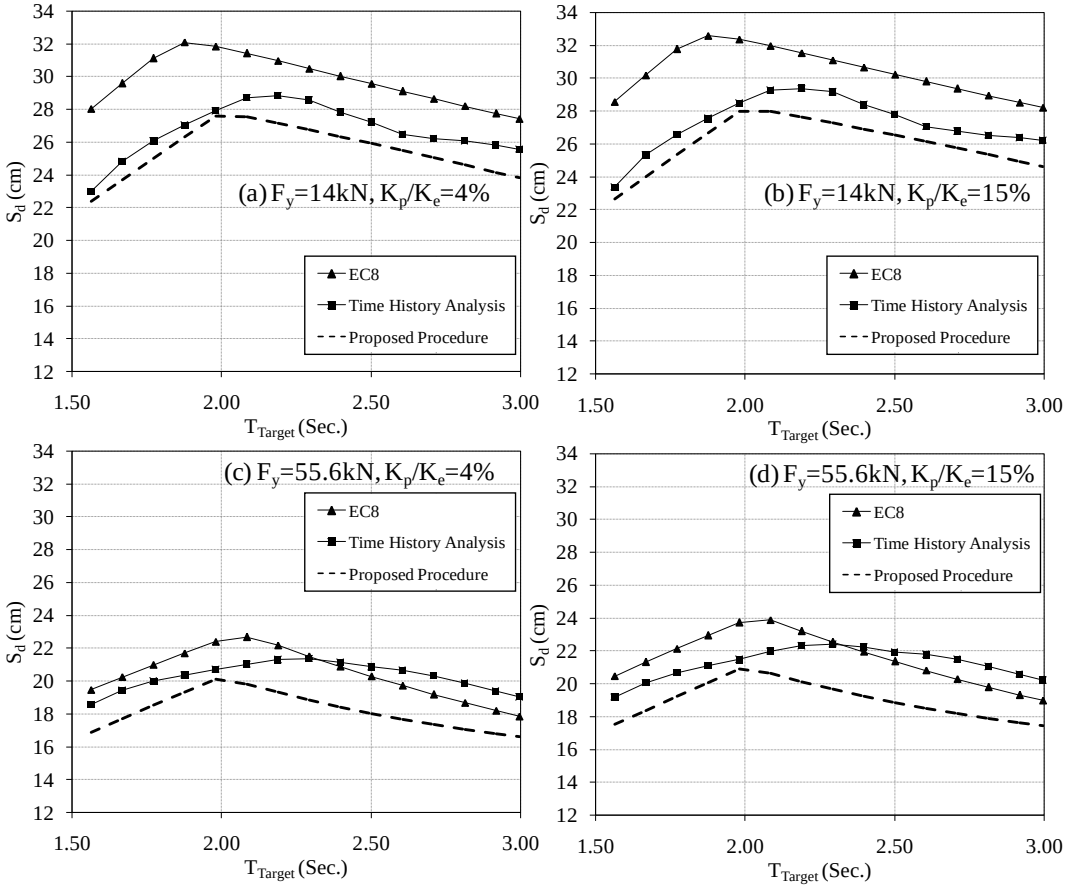

Fig. 13 The proposed procedure displacement verification against EC8 and time history analysis for: (a) F_y=14 kN, and K_p/K_e=4%; (b) F_y=14 kN, and K_p/K_e=15%; (c) F_y=55.6 kN, and K_p/K_e=4%; and (d) F_y=55.6 kN, and K_p/K_e=15%

setup of Xing *et al*. (2012) is considered matching the assumptions of the proposed procedure as a single degree of freedom system; consequently, the obtained force (with error around 9.85%) is in better agreement compared with the numerical test of Kilar and Koren (2009). According to the introduced verifications, it is worth noting that the proposed procedure can be applied to both concrete and steel base-isolated structures, once the aforementioned procedure assumptions are satisfied.

4. Conclusions

A comparison has been conducted to evaluate eight different methods, contributing in the literature of seismic design codes, for calculating the force reduction factor due to damping. Accordingly, a simplified seismic analysis procedure has been proposed based on the well documented N2 method. Direct application and verification of the proposed procedure has been performed and the main conclusions can be summarized as follows:

1. Any of the discussed methods in the literature can be employed in the proposed procedure for damping modification.

2. It is evident that the damping modification factor has a range of 1.25 to 2.5 for a damping ratio in a range of 10% to 50%. This is consistent with the range specified in different seismic design codes (UBC-97, IBC-2009, FEMA-356, and EC8) in between 1.5 to 2.0 for the common lateral load resisting systems of base-isolated structures.

3. The results of the proposed procedure are in good agreement with those of the nonlinear time history analysis and EC8. In addition, the results have been verified against those of numerical and experimental investigations in the literature.

4. The proposed procedure can be applied to both concrete and steel base-isolated structures, once the procedure assumptions are satisfied.

5. The isolation post-yield stiffness to elastic stiffness ratio (K_p/K_e) has negligible effect on both the effective stiffness and the effective damping of the isolation system. Accordingly, it has negligible effect on both the design force and the design displacement of the system.

6. The yield level of the isolation (F_y) affects both the effective stiffness and the effective damping of the system. Accordingly, it affects the induced design force and design displacement that decrease as the yield level increases.

References

Ashour, S.A. and Hanson, R.D. (1987), "Elastic seismic response of buildings with supplemental damping", Report UMCE 87-1, Department of Civil Engineering, The University of Michigan, Ann Arbor, Michigan.

ATC-40 (1996), *Seismic Evaluation and Retrofit of Concrete Building*, Applied Technology Council, Redwood City, CA.

Bommer, J.J., Elnashai, A.S. and Weir, A.G. (2000), "Compatible acceleration and displacement spectra for seismic design codes", *Proceedings of the 12th World Conference on Earthquake Engineering*.

Bommer, J. and Mendis, R. (2005), "Scaling of spectral displacement ordinates with damping ratios", *Earthq. Eng. Struct. Dyn.*, **34**(2), 145-165.

Chao, X., Geoffrey, J. and Geoffrey, W. (2014), "Physical parameter identification of nonlinear base-isolated buildings using seismic response data", *Comput. Struct.*, **145**, 47-57.

El-Gazzar, S. (2013), "Simplified seismic analysis procedure for base isolated structures", MSc. Thesis, Struct. Eng. Department, Cairo University.

Fajfar, P. and Eeri, M. (2000), "A nonlinear analysis method for performance based seismic design", *Earthq. Spectra*, **16**(3), 573-592.

FEMA 273 (1997), "NEHRP guidelines for the seismic rehabilitation of buildings", *The Federal Emergency Management Agency*, Washington, DC.

FEMA 356 (2000), "Prestandard and commentary for the seismic rehabilitation of buildings", *The Federal Emergency Management Agency*, 1801 Alexander Bell Drive, Reston, Virginia.

Hatzigeorgiou, G. (2010), "Damping modification factors for SDOF systems subjected to near-fault and artificial earthquakes", *Earthq. Eng. Struct. Dyn.*, **39**(11), 1239-1258.

Iervolino, I., Galasso, C. and Cosenza, E. (2010), "REXEL: Computer aided record selection for code-based seismic structural analysis", *Bull. Earthq. Eng.*, **8**(2), 339-362.

Kawashima, K. and Aizawa, K. (1986), "Modification of earthquake response spectra with respect to damping ratio", *Proceedings of the 3rd US National Conference on Earthquake Engineering*, Charleston, SC.

Kelly, T. (2001), *Base Isolation of Structures Design Guidelines*, Holmes consulting group Ltd, Wellington, New Zealand.

Kilar, V. and Koren, D. (2008), "Usage of simplified N2 method for analysis of base isolated structures", *The 14th World Conference on Earthquake Engineering*, Beijing, China.
Kilar, V. and Koren, D. (2009), "Simplified inelastic seismic analysis of base isolated structures using the N2 method", *Earthq. Eng. Struct. Dyn.*, **39**(9), 967-989.
Leblouba, M. (2012), "Response spectrum analysis for regular base isolated buildings subjected to near fault ground motions", *Struct. Eng. Mech.*, **43**(4), 527-543.
Lee, D.G., Hong, J.M. and Kim, J. (2001), "Vertical distribution of equivalent static loads for base isolated building structures", *Eng. Struct*., **23**(10), 1293-1306.
Lin, Y. and Chang, K. (2003), "A study on damping reduction factor for buildings under earthquake ground motions", *J. Struct. Eng*., **129**(2), 206-214.
Lin, Y., Miranda, M. and Chang, K. (2005), "Evaluation of damping reduction factors for estimating elastic response of structures with high damping", *Earthq. Eng. Struct. Dyn.*, **34**(11), 1427-1443.
Ma, C., Zhang, Y., Zhao, Y., Tan, P. and Zhou, F. (2011), "Stochastic seismic response analysis of base-isolated high-rise buildings", *Procedia Eng.*, **14**, 2468-2474.
Murat, D. and Srikanth, B. (2007), "Comprehensive evaluation of equivalent linear analysis method for seismic-isolated structures represented by SDOF systems", *Eng. Struct.*, **29**(8), 1653-1663.
Naeim, F. and Kelly, J. (1999), *Design of Seismic Isolated Structures from Theory to Practice*, John Wiley & Sons, NY.
Newmark, N. and Hall, W. (1982), *Earthquake Spectra and Design*, EERI Monograph series, Earthquake engineering research institute, Oakland, CA.
Nicos, M. and Georgios, K. (2013), "The engineering merit of the effective period of bilinear isolation systems", *Earthq. Struct.*, **4**(4), 397-428.
Palazzo, B. and Petti, L. (1996), "Reduction factors for base isolated structures", *Comput. Struct.*, **60**(6), 945-956.
Priestley, M.J.N. and Grant, D.N. (2005), "Viscous damping for analysis and design", *J. Earthq. Eng.*, Special Edition.
Ramirez, O., Constantinou, M., Kircher, C., Whittaker, A., Johnson, M., Gomez, J. and Chrysostomou, C. (2002), "Elastic and inelastic seismic response of buildings with damping systems", *Earthq. Spectra*, **18**(3), 531-547.
Sadek, F., Mohraz, B. and Riley, M. (2000), "Linear procedures for structures with velocity dependent dampers", *J. Struct. Eng*., ASCE, **126**(8), 887-895.
Takewaki, I. (2011), *Building Control with Passive Dampers: Optimal Performance-based Design for Earthquakes*, John Wiley & Sons.
Tao, L., Tobia, Z., Bruno, B. and Qilin, Z. (2014a), "Evaluation of equivalent linearization analysis methods for seismically isolated buildings characterized by SDOF systems", *Eng. Struct*., **59**, 619-634.
Tao, L., Tobia, Z., Bruno, B. and Qilin, Z. (2014b), "An improved equivalent linear model of seismic isolation system with bilinear behavior", *Eng. Struct*., **61**, 113-126.
Tobia, Z., Tao, L., Bruno, B. and Qilin, Z. (2014), "Improved equivalent viscous damping model for base-isolated structures with lead rubber bearings", *Eng. Struct*., **75**, 340-352.
Tolis, S.V. and Faccioli, E. (1999), "Displacement design spectra", *J. Earthq. Eng.*, **3**(01), 107-125.
Varnavas, V. and Petros, K. (2013), "Assessing the effect of inherent nonlinearities in the analysis and design of a low-rise base isolated steel building", *Earthq. Struct*., **5** (5), 499-526.
Wu, J. and Hanson, R. (1989), "Inelastic response spectra with high damping", *J. Struct. Div*., ASCE, **115**(6), 1412-1431.
Xing, C., Wang, H., Li, A. and Wu, J. (2012), "Design and experimental verification of a new multi-functional bridge seismic isolation bearing", *J. Zhejiang University Science A*, **13**(12), 904-914.

Notations

a_a, a	Numerical coefficients
a_g	Earthquake ground acceleration
A_h	Area of the hysteresis loop (the energy dissipated per cycle)
B	Damping modification factor
B_a	Acceleration damping modification factor - ADMF.
b_a	Numerical coefficient
B_d	Displacement damping modification factor - DDMF.
B_s	Damping coefficient associated with the short period of vibration
B_1	Damping coefficient associated with period of vibration 1.0 Sec.
C_1, C_2, C_3, C_4, C_5	Numerical coefficients
F_m	Design force of the system
F_y	Yield strength of the system
g	Gravity acceleration
K_{eff}	Effective stiffness
K_e	Elastic stiffness
K_p	Post-yield stiffness
M	Total mass of the system.
Q	Characteristic shear strength of the isolation system
R	Force reduction factor (response modification factor)
R_α	Ductility force reduction factor with positive post-yield stiffness
R_μ	Ductility force reduction factor with zero post-yield stiffness
S	Local soil coefficient in design codes
S_a	Spectral acceleration – elastic or inelastic
S_{ae}	Elastic spectral acceleration
S_{ay}	Spectral acceleration at the yield strength of the system
S_{ap}	Spectral acceleration at a post-yield state of the system
S_d	Spectral displacement – elastic or inelastic
S_{de}	Elastic spectral displacement
S_{dy}	Spectral displacement at the yield strength of the system
S_{dp}	Spectral displacement at a post-yield state of the system
T_{eff}	Effective vibration period
T	Natural vibration period
T_B,T_C,T_D,T_E,T_F,T_S	Characteristic vibration periods of the response spectrum
ζ	Viscous damping ratio
α	Post-yield stiffness to elastic stiffness ratio
α_a	Numerical Coefficient
ξ_{eff}	Effective viscous damping ratio
μ	Ductility demand
ψ	Response parameter